Quantum mechanical model for Rutherford backscattering of ion beams by thin crystalline lattices

J. L. den Besten

Microanalytical Research Center, School of Physics, University of Melbourne, Parkville, Victoria 3052, Australia

L. J. Allen

School of Physics, University of Melbourne, Parkville, Victoria 3052, Australia

D. N. Jamieson

Microanalytical Research Center, School of Physics, University of Melbourne, Parkville, Victoria 3052, Australia

During the 1960s there was much discussion about the transition from a quantal to a classical description of ion-beam channeling. There is no reason why a quantal model should not be used. However, no such calculations have been attempted. We present a fully quantum mechanical model for Rutherford backscattering of an ion beam from a thin crystalline lattice. Good agreement with experimental Rutherford backscattering angular scans is demonstrated. The transition from the quantal to the classical model is discussed.
[S0163-1829(99)04729-3]

I. INTRODUCTION

Beams of charged particles are routinely used for structural characterization of materials. Nuclear microprobes and electron microscopes are now standard analytical tools for structural analysis at the atomic level that can provide information on elemental composition and impurity concentrations within a sample.[1] We will concentrate on thin crystalline samples where information on the structure and on the site distribution of impurities can be obtained. An experimental technique that is common to both ion-beam and electron microanalysis is Rutherford backscattering (RBS). The RBS yield, as a function of orientation of an incident electron beam, can now be accurately calculated from first principles within the framework of quantum mechanical dynamical diffraction theory.[2] On the other hand, for incident ions the scattering yield is usually calculated using classical principles and concepts in ion channeling first proposed by Lindhard and co-workers.[3,4] Monte Carlo simulation is the most flexible and reliable method based on classical mechanics for simulation of these light ion phenomena.[5]

The differences between ion and electron interactions with a given single crystal are due to charge and mass. Ions are repelled by the atoms in the crystals while electrons are attracted. At a given energy the de Broglie wavelength of ions is much less than for electrons. For example, the de Broglie wavelength of 1 MeV electrons is 8.7×10^{-3} Å and that for protons is 2.9×10^{-4} Å, a factor of 30 less. A quantal (diffraction) description of 1 MeV electrons is essential.[6] An order-of-magnitude reduction in the de Broglie wavelength for 1 MeV protons would suggest that quantal effects could still be of considerable importance.

The issue of a classical versus quantal description of ion-beam channeling in crystals and the transition to the classical limit was extensively discussed in the 1960s. However, largely due to computational limitations, no attempt was ever made to do a realistic, fully quantal, many beam diffraction calculation of ion-beam channeling phenomena. Chadderton[7] has suggested that the star patterns seen in transmission of ions through single crystals are the analog of the Kikuchi patterns, which arise in electron diffraction (from thicker crystals). Kikuchi bands are a consequence of the fact that inelastically scattered electron waves are subject to the processes of Bragg reflection and anomalous absorption.

In terms of a wave model, the Ewald sphere construction[8] shows that many more diffracted beams are excited for the smaller wavelength or larger wave number associated with MeV ions. The Bragg angle also decreases and the features on a diffraction pattern shrink inwards towards the central transmitted beam. This means that, even with a well collimated and monoenergetic incident beam, diffraction spots would be extremely difficult to observe in ion-beam channeling (from a thin crystal, where absorptive scattering does not dominate the transmission pattern). Nevertheless, although the scattering may appear classical and classical models give a reasonable description of RBS, this does not mean that diffraction of the incident ions is not occurring. In this quantal approach the scattering mechanism is treated quantitatively. It is shown in this paper that the large number of Bloch waves and small Bragg angles together with the smoothing effect of inelastic (absorptive) scattering, which is important for light ions, give rise to scattering which looks *effectively* like classical scattering. However, this approach allows the quantitative determination of the relative sizes of independent effects on an RBS scattering experiment.

In this paper we introduce a model for ion-beam channeling based on a fully quantum mechanical treatment using Bloch waves. It is, in some respects, analogous to that used with success to model electron channeling.[8,9] This model allows us to quantitatively predict RBS channeling angular scans from first principles. RBS, where we can restrict ourselves to small effective thicknesses of the order of a thousand angstroms (by monitoring energy loss) is ideal for a test of our diffraction model. This is because the short mean free

path for inelastic scattering in crystals (relative to electrons) means that coherent elastic dynamical diffraction can only be important in the first few hundred angstroms of a crystal.

II. DYNAMICAL DIFFRACTION THEORY

The collision of an ion with a crystalline slab is a many body problem. However, to a good approximation, we will describe the collision as scattering of the incident ion in the potential field of the crystal. The wave function describing the ion is obtained by solving the Schrödinger equation

$$\nabla^2 \psi(\mathbf{r}) + \frac{2m}{\hbar^2}[E + V(\mathbf{r}) + iW(\mathbf{r})]\psi(\mathbf{r}) = 0, \qquad (1)$$

where m is the reduced mass of the system, $V(\mathbf{r})$ is the potential associated with elastic scattering and the potential term $W(\mathbf{r})$ represents absorptive scattering. The spatial distribution of $V(\mathbf{r})$ and $W(\mathbf{r})$ are given by the Fourier expansions

$$V(\mathbf{r}) = \sum_{\mathbf{g}} V_{\mathbf{g}} \exp(i\mathbf{g}\cdot\mathbf{r}) \quad \text{and} \quad W(\mathbf{r}) = \sum_{\mathbf{g}} W_{\mathbf{g}} \exp(i\mathbf{g}\cdot\mathbf{r}), \qquad (2)$$

where $V_{\mathbf{g}}$ and $W_{\mathbf{g}}$ are the Fourier coefficients of the potentials and the $\mathbf{g}$ are reciprocal lattice vectors. In practice the sums over all reciprocal lattice vectors are truncated to a subset of the physically important ones. Consistent with the periodic nature of the potentials, we assume that the wave function of the incident ion in the crystal, taking absorptive scattering into account, may be described as a linear superposition of Bloch states, with complex wave vectors $\mathbf{K} + \lambda^i \hat{\mathbf{n}}$, such that[9]

$$\psi(\mathbf{K},\mathbf{r}) = \sum_i \alpha^i \sum_{\mathbf{g}} C_{\mathbf{g}}^i \exp[i(\mathbf{K} + \lambda^i\hat{\mathbf{n}} + \mathbf{g})\cdot\mathbf{r}] = \sum_i \alpha^i \phi^i(\mathbf{r}), \qquad (3)$$

where the wave vector $\mathbf{K}$ in the crystal is corrected for refraction, i.e., $K^2 = k^2 + (2m/\hbar^2)V_0$, with k as the wave number. The unit vector $\hat{\mathbf{n}}$ is an inwardly directed surface normal. Here α^i is the excitation amplitude of the ith Bloch state $\phi^i(\mathbf{r})$. The α^i and the coefficients $C_{\mathbf{g}}^i$ and λ^i are obtained by substituting Eqs. (2) and (3) into Eq. (1) to obtain the dynamical scattering equations of Bethe,[10]

$$[K^2 - (\mathbf{K} + \lambda^i\hat{\mathbf{n}} + \mathbf{g})^2]C_{\mathbf{g}}^i + \frac{2m}{\hbar^2}\sum_{\mathbf{h}} (V_{\mathbf{g}-\mathbf{h}} + iW_{\mathbf{g}-\mathbf{h}})C_{\mathbf{h}}^i = 0. \qquad (4)$$

Assuming that $K \approx k$ and that $K \gg g$ we can recast Eq. (4) in the form of an eigenvalue problem.[8,9] Then the Bloch state coefficients $C_{\mathbf{g}}^i$ in Eq. (3) are just the components of the eigenvector corresponding to a complex eigenvalue $\lambda^i = \gamma^i + i\eta^i$. The real part of the eigenvalue γ^i is usually called the *anpassung* and maps out the elastic dispersion surface, and the imaginary part η^i is the absorption coefficient.

The Fourier coefficients in Eq. (2) of the periodic crystal potential leading to elastic scattering are given by[8]

$$V_{\mathbf{g}} = \frac{4\pi}{V_c}\sum_n \exp[-M_n(\mathbf{g})]$$
$$\times \exp(-i\mathbf{g}\cdot\mathbf{r}_n)\int_0^\infty r^2 V_n(r)\frac{\sin(gr)}{gr}dr, \qquad (5)$$

where V_c is the volume of a unit cell, $\mathbf{r}_n$ is the lattice site of atom n in the unit cell, $M_n(\mathbf{g}) = \frac{1}{2}g^2\langle u_n^2\rangle$ is the Debye-Waller factor for atom n and takes into account the thermal motion of the atom via the projected mean-square thermal displacement $\langle u_n^2\rangle$. The ion-atom potential $V_n(r)$ for scattering from atom n in the unit cell can be represented in the form

$$V_n(r) = \frac{ZZ_ne^2}{4\pi\epsilon_0 r}\Phi(r/a_n), \qquad (6)$$

where r is the distance between the incoming ion and the atom n. Z and Z_n are the atomic numbers of the incident ion and atom n, respectively, and Φ is a screening function, which depends on the screening length a_n. A commonly used form for Φ is the universal screening function which is of the form

$$\Phi(r/a_n) = \sum_{j=1}^{4} A_j \exp(-B_j r/a_n), \qquad (7)$$

where the screening length a_n is given by $a_n = 0.8853a_0/(Z^{0.23} + Z_n^{0.23})$, a_0 the Bohr radius, and the parameters A_j and B_j are given in Ref. 11. For the ion-atom interaction given by Eq. (6) this gives

$$V_{\mathbf{g}} = \frac{4\pi\hbar^2 Z}{m_e a_0 V_c}\sum_n Z_n \exp[-M_n(\mathbf{g})]$$
$$\times \exp(-i\mathbf{g}\cdot\mathbf{r}_n)\sum_j \frac{A_j}{(B_j/a_n)^2 + g^2}, \qquad (8)$$

where m_e is the rest mass of the electron.

III. THE SCATTERING CROSS SECTION

The incorporation of the absorptive part of the crystal potential in Eq. (1), the Schrödinger equation, leads to a rate of flux loss per unit volume, at the point $\mathbf{r}$, proportional to $W(\mathbf{r})|\psi(\mathbf{r})|^2$, see, e.g., Ref. 12. The absorption cross section for a crystal of volume V is given by

$$\sigma = \frac{2m}{\hbar^2 k}\int_V W(\mathbf{r})|\psi(\mathbf{r})|^2 d^3\mathbf{r}. \qquad (9)$$

If we assume that the contribution to $W(\mathbf{r})$ from different absorptive processes is additive, then we can obtain the cross section for a single such process, such as RBS, by retaining just the appropriate term $W^{RBS}(\mathbf{r})$ in $W(\mathbf{r})$ in Eq. (9). However, note that in $|\psi(\mathbf{r})|^2$ the effect of all absorptive processes must still be taken into account.

We can express the volume of the crystal as $V = NV_c$, N the number of unit cells. Using the Fourier expansion of $W^{RBS}(\mathbf{r})$ and Eq. (3) we can write the cross section for scattering from the crystal, due to ions undergoing dynamical diffraction, in the form[2,13,14]

TABLE I. Summary of the essential parameters for the planar channeling cases considered in this paper. The first three columns give the incident ion, its energy (E) and the corresponding de Broglie wavelength (λ). The next three columns give the target crystal, the plane used to obtain the RBS channeling map, and the interplanar spacing (d). Then follow the number of beams used in the calculation of the RBS cross section (N), the effective depth of the crystal for RBS (t), the temperature of the crystal, and the corresponding projected mean-square thermal displacements ($\langle u_i^2 \rangle$). The mean free path of the mean absorption is given for those cases where this has been considered in the calculations (λ_{abs}). The convergence semiangle of the incident beam, where taken into account, is shown next (θ_{con}). Last, the source of each set of experimental data is shown.

Ion	E (MeV)	λ ($\text{Å} \times 10^{-4}$)	Cryst.	Plane	d (Å)	N	t (Å)	Temp. (K)	$\langle u_i^2 \rangle$ ($\text{Å}^2 \times 10^{-2}$)	λ_{abs} (Å)	θ_{con} (deg)	Ref.
^{4}He	1.0	1.4	Ge	{110}	2.00	251	600	293	0.72	2000	.08	16
p	1.7	2.2	MgO	{100}	1.49	201	2500	293	0.47 (Mg)		.04	18
									0.42 (O)			
				{110}	2.10							
	.008	32	Ni	{110}	1.25	101	100	293	0.47	500	.10	19

$$\sigma_{dyn} = N V_c \frac{2m}{\hbar^2 k} \sum_{i,j} B^{ij}(t) \sum_{\mathbf{g},\mathbf{h}} C_{\mathbf{g}}^i C_{\mathbf{h}}^{j*} W_{\mathbf{h}-\mathbf{g}}^{RBS}, \qquad (10)$$

where

$$B^{ij}(t) = \alpha^i \alpha^{j*} \frac{\exp[i(\lambda^i - \lambda^{j*})t] - 1}{i(\lambda^i - \lambda^{j*})t}. \qquad (11)$$

This expression gives the contribution to the RBS cross section from ions which are channeling. It incorporates the phenomenon of flux peaking which is usually treated independently of the scattering cross section in the classical approach. The decrease in Bloch wave intensities due to dechanneling leads to a diffuse background of ions which can also undergo RBS. We take this contribution into account by adding a term of the form[13,14]

$$\sigma_{dif} = N V_c \frac{2m}{\hbar^2 k} \left[1 - \sum_{i,j} B^{ij}(t) \sum_{\mathbf{g}} C_{\mathbf{g}}^i C_{\mathbf{g}}^{j*} \right] W_{\mathbf{0}}^{RBS}. \qquad (12)$$

We can express the Fourier coefficients of $W^{RBS}(\mathbf{r})$ in the form

$$W_{\mathbf{h}-\mathbf{g}}^{RBS} = \sum_n \exp[-M_n(\mathbf{h}-\mathbf{g})]\exp[-i(\mathbf{h}-\mathbf{g}) \cdot \mathbf{r}_n] \nu_{\mathbf{h}-\mathbf{g}}^n, \qquad (13)$$

where $\nu_{\mathbf{h}-\mathbf{g}}^n$ is effectively a Fourier coefficient of an atomic form factor [cf. Eqs. (5) and (8)]. Since the ion-atom interaction leading to RBS is highly localized on the atomic sites, we will assume that $W^{RBS}(\mathbf{r})$ can be represented by delta functions, smeared by the thermal motion of the atoms, located on each atomic site. This means we make the approximation $\nu_{\mathbf{g}}^n \approx \nu_{\mathbf{0}}^n$ for all $\mathbf{g}$, so that

$$W_{\mathbf{h}-\mathbf{g}}^{RBS} \approx \sum_n \exp[-M_n(\mathbf{h}-\mathbf{g})]\exp[-i(\mathbf{h}-\mathbf{g}) \cdot \mathbf{r}_n] \nu_{\mathbf{0}}^n. \qquad (14)$$

Note that $\nu_{\mathbf{0}}^n$ is proportional to Z_n^2. The total RBS cross section becomes

$$\sigma = N V_c \frac{2m}{\hbar^2 k} \sum_n \nu_{\mathbf{0}}^n \left\{ \left[1 - \sum_{i,j} B^{ij}(t) \sum_{\mathbf{g}} C_{\mathbf{g}}^i C_{\mathbf{g}}^{j*} \right] \right.$$

$$+ \sum_{i,j} B^{ij}(t) \sum_{\mathbf{g},\mathbf{h}} C_{\mathbf{g}}^i C_{\mathbf{h}}^{j*} \exp[-M_n(\mathbf{h}-\mathbf{g})]$$

$$\left. \times \exp[-i(\mathbf{h}-\mathbf{g}) \cdot \mathbf{r}_n] \right\}. \qquad (15)$$

The term in curly brackets arises from the periodic structure of the lattice and is the depth-averaged ion probability density on the atomic site labeled by $\mathbf{r}_n$. The summation is over all atomic sites in the unit cell. Therefore, as expected, an experiment in which the crystal is tilted and the RBS yield observed as a function of orientation is effectively an experiment in which the change in particle probability density at the atomic sites is monitored. In an amorphous solid the term in curly brackets becomes one.
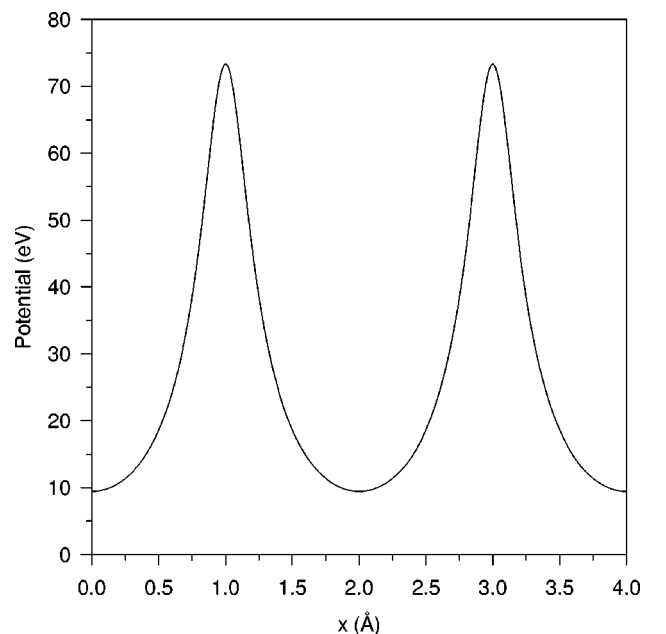
FIG. 1. Potentials for the elastic scattering of 1.0-MeV ^{4}He ions from the {110} plane in Ge. The maxima correspond to the positions of Ge atoms. Thermal corrections are included.
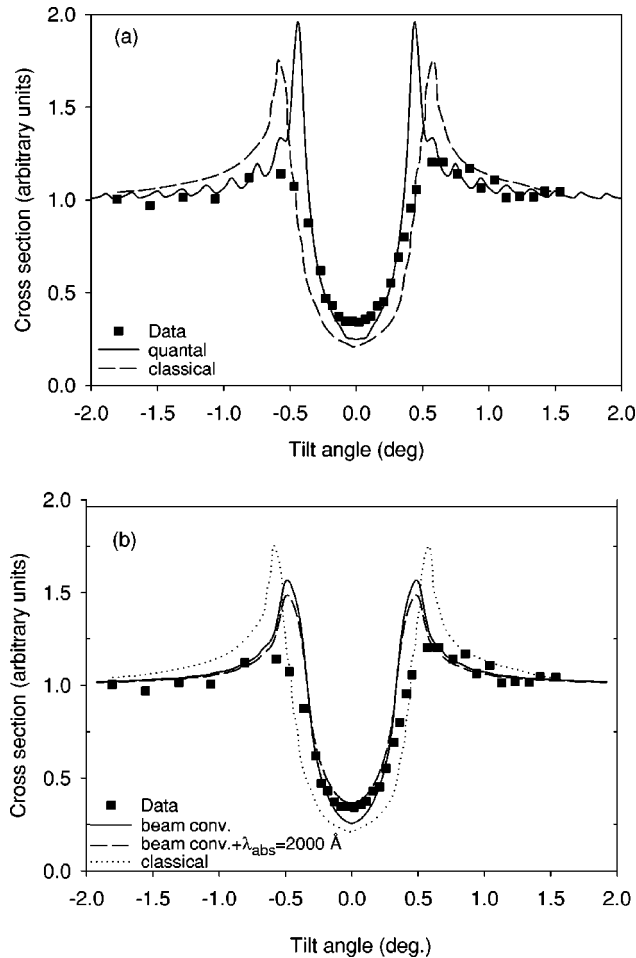
FIG. 2. RBS cross sections for 1.0-MeV ^{4}He ions as a function of crystal tilt with respect to the center of the {110} plane in Ge at 293 K. The calculations are for scattering to a depth of 600 Å. In (a) the quantal result is compared to the data and classical calculation from Ref. 16. In (b) a convergence semiangle of 0.08° for the incident beam is applied to the quantal result and also the addition of a mean absorption with a mean free path $\lambda_{abs} = 2000$ Å.

IV. EXAMPLES

We have calculated the cross section for RBS as a function of the orientation of the incident beam relative to the crystal for several cases where experimental data exist. We restrict ourselves to planar cases since fully converged calculations with respect to the number of beams (reciprocal-lattice vectors) used requires of the order of 200 beams, an order of magnitude more than would be needed in high-energy electron diffraction. To obtain convergence for similar zone axis cases would require approximately 200×200 beams, which is computationally demanding since the calculations scale as the number of beams cubed. The examples here have utilized sufficient beams to provide convergence but they are not necessarily the minimum number required.

Our examples have been chosen to cover a wide range of energies and the cases of both incident proton and helium ions. The essential parameters are summarized in Table I.

The first case considered is the scattering of 1.0 MeV ^{4}He ions undergoing RBS from a Ge crystal for the {110} planar case. The potential for elastic scattering was constructed as described in Sec. II. The projected mean-square thermal dis-
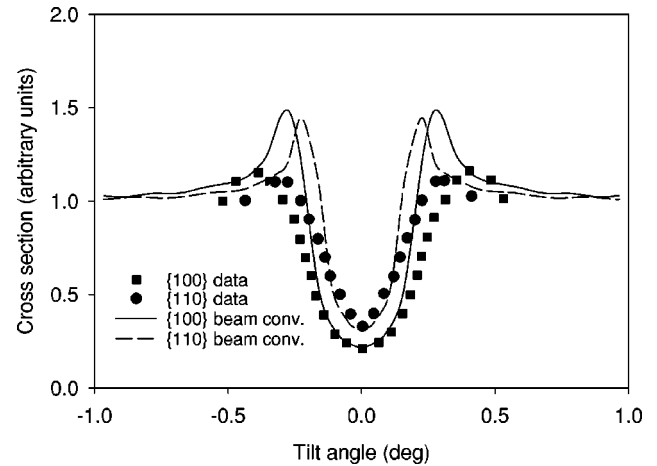
FIG. 3. RBS cross sections for 1.7-MeV protons as a function of crystal tilt with respect to the center of the {100} and {110} planes in MgO at 293 K. The calculations are for scattering to a depth of 2500 Å in each case. The data are from Ref. 18. The calculated results take into account a convergence semiangle of 0.04° for the incident beam.

placement in Table I was taken from Ref. 15. The potential, corrected for the thermal motion of the atoms, is shown in Fig. 1. On the scale of this figure it is almost indistinguishable from that obtained using the continuum model for planes of atoms.[3] This is an important factor in the close agreement between this quantal formulation and the classical models. The potential in Fig. 1 took less than one minute of CPU time to calculate on a 233 MHz Dec Digital Alphastation. Shown in Fig. 2 are RBS cross sections as a function of crystal tilt with respect to the center of the {110} plane. The calculations are for scattering to a depth of 600 Å, consistent with the experiment of Picraux and Anderson.[16] Experimental counts are just related to the cross section for the crystal by a factor which is the product of the beam current density and the measurement time, assumed constant for each orientation. In Fig. 2(a) the quantal result is compared to the data and classical calculation from Ref. 16. Notice the fine structure in the quantal result which is not present in the classical calculation. In Fig. 2(b) a convergence semiangle of 0.08° for the incident beam is applied to the quantal result and then the effect of also including a mean absorption potential W_0 with a mean free path $\lambda_{abs} = 2000$ Å in the calculations is shown. This leads to a smoothing of the quantal result and gives good agreement between theory and experiment, except in the shoulder region. This suggests that a more sophisticated absorption correction which depends on orientation is required, rather than the mean overall absorption we have applied. The calculation of the quantal cross section shown in Fig. 2(a) took 114 min on the same 233 MHz Alphastation for 101 different tilt-angle values, that is, roughly 1 min per tilt angle.

The next case we have considered is that of 1.7 MeV protons scattered from an MgO crystal for both the {100} and {110} planar cases. Thermal effects were taken into account using the mean-square thermal displacements from Ref. 17 shown in Table I. RBS cross sections are shown in Fig. 3 where they are compared to data from Ref. 18. The calculated results take into account a convergence semiangle of 0.04° for the incident beam. The depth and width of the
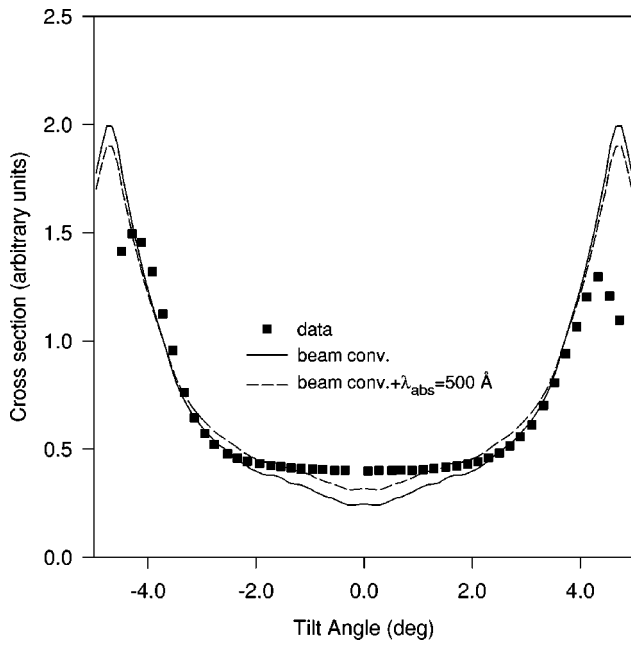
FIG. 4. RBS cross sections for 8.0 keV protons as a function of crystal tilt with respect to the center of the {100} plane in Ni at room temperature. The calculations are for scattering to a depth of 100 Å. The data are from Ref. 19. The calculated results take into account a convergence semiangle of 0.1° for the incident beam and then also the addition of a mean absorption with a mean free path λ_{abs} = 500 Å.

channel are correctly reflected in each case but, once again, the theory predicts larger values of the cross section in the shoulder region.

Last, we have considered data taken for incident protons at the much lower energy of 8 keV. RBS cross sections as a function of crystal tilt with respect to the center of the {100} plane in Ni at room temperature are shown in Fig. 4. The data are from Ref. 19. The projected mean-square thermal displacement in Table I was taken from Ref. 15. The calculated results take into account a convergence semiangle of 0.1° for the incident beam and the effect of also including a
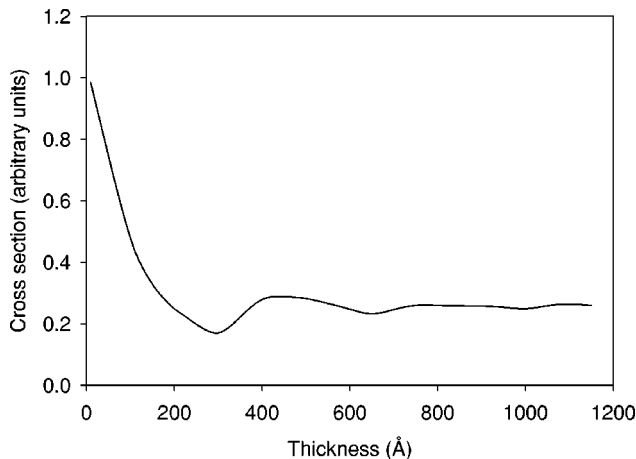
FIG. 5. RBS cross sections for 1.0-MeV ^{4}He ions incident parallel to the {110} planes in Ge at 293 K. The calculations are for scattering to a range of depths up to nearly 1200 Å. No account was taken of beam convergence. No mean absorption was included.
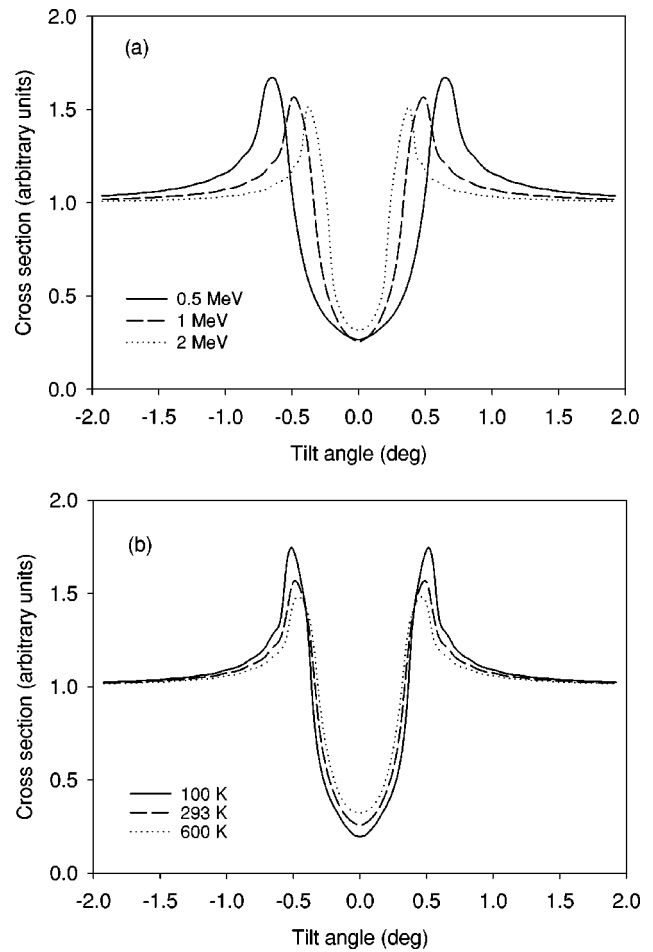
FIG. 6. RBS cross sections for incident ^{4}He ions as a function of crystal tilt with respect to the center of the {110} plane in Ge. The calculations are for scattering to a depth of 600 Å. The convergence semiangle of the incident beam was assumed to be 0.08°. No mean absorption was included. In (a) we show the cross section as a function of incident beam energy at 293 K. In (b) the cross section is given as a function of sample temperature for an incident energy of 1.0 MeV.

mean absorption with a mean free path λ_{abs} = 500 Å is illustrated. Once again the predicted width and depth of the angular scan are excellent but the experimental points are below the theoretical predictions in the shoulder region.

In general we found our calculations of RBS cross sections to be relatively insensitive to thickness in the vicinity of the values used for proton scattering. However, for 1.0 MeV He ions scattered from Ge at 239 K there was a strong depth dependence in the vicinity of 600 Å. In Fig. 5 we show the RBS cross section for a beam aligned parallel to the crystal planes (i.e., a tilt angle of zero) for a range of depths to nearly 1200 Å. Thereafter the cross section was found to be insensitive to thickness. As before, thermal corrections were included. However, no account was taken of beam convergence and no mean absorption was included in the calculations. Our model clearly shows the oscillations in the backscattering yield as a function of the thickness of the crystal. The oscillations display several maxima as the crystal increases in thickness with a period of roughly 400 Å and which are damped as the thickness increases. In the classical model, these oscillations arise from the correlated nature of

the trajectories of the incident ions as they enter the crystal. For a beam aligned with the crystal planes, the extrema of the oscillation amplitude relative to the middle of the gap between the atom planes increases the close encounter probability with the ion strings and hence the backscattered yield from those thicknesses is enhanced.[20] This arises from our model without any special refinement.

It is also interesting to see whether our model predicts a reasonable behavior for the cross sections as a function of incident energy. It is also well known that the temperature of the sample has an effect on the RBS angular scans. In Fig. 6(a) we show the cross section as a function of incident beam energy for [4]He ions on Ge as a function of crystal tilt with respect to the center of the {110} plane at 293 K. The effective depth is 600 Å and the convergence semiangle of the incident beam was assumed to be 0.08°. No mean absorption was included. The width of the RBS channeling map increases with increasing energy while the depth is constant. This is consistent with classical models. In Fig. 6(b) the cross section is given as a function of sample temperatures between 100 and 600 K for an incident energy of 1.0 MeV. The channel effectively becomes less narrow and less deep

as the temperature increases. Once again this is consistent with the predictions of classical models.

V. CONCLUSIONS

We have presented a fully quantum mechanical model for RBS of ion beams from a thin crystalline lattice. The approach is similar to that which has been extremely successful for electron channeling. Good agreement with experimental RBS planar channeling maps has been demonstrated for different incident ions and energies and different crystals with respect to the channel's minimum depth and width. Further investigation into the orientation dependence of channeling in the crystal requires a more detailed treatment of absorption to obtain a better agreement with experiment in the shoulder region of the RBS channeling maps. We intend to extend our calculations to the two-dimensional, axial case.

[1] M. B. H. Breese, D. N. Jamieson, and P. J. C. King, *Materials Analysis Using a Nuclear Microprobe* (Wiley, New York, 1996).

[2] C. J. Rossouw, P. R. Miller, T. W. Josefsson, and L. J. Allen, Philos. Mag. A **70**, 985 (1994).

[3] J. Lindhard, Mat. Fys. Medd. K. Dan. Vidensk. Selsk. **34**, No. 14, 1 (1965).

[4] D. S. Gemmel, Rev. Mod. Phys. **46**, 129 (1974).

[5] J. H. Barret, Nucl. Instrum. Methods Phys. Res. B **44**, 367 (1990).

[6] J. M. Cowley, *Diffraction Physics*, third revised ed. (Elsevier, Amsterdam, 1995).

[7] L. T. Chadderton, in *Channeling—Theory Observations and Applications*, edited by D. V. Morgan (Wiley, London, 1973), p. 287.

[8] C. J. Humphreys, Rep. Prog. Phys. **42**, 1825 (1979).

[9] L. J. Allen and C. J. Rossouw, Phys. Rev. B **39**, 8313 (1989).

[10] H. Bethe, Ann. Phys. (Leipzig) **87**, 55 (1928).

[11] D. J. O'Connor and J. P. Biersack, Nucl. Instrum. Methods Phys. Res. B **15**, 14 (1986).

[12] H. D. Heidenreich, J. Appl. Phys. **33**, 2321 (1962).

[13] L. J. Allen and C. J. Rossouw, Phys. Rev. B **47**, 2446 (1993).

[14] L. J. Allen and T. W. Josefsson, Phys. Rev. B **52**, 3184 (1995).

[15] N. M. Butt, J. Bashir, B. T. M. Willis, and G. Heger, Acta Crystallogr., Sect. A: Found. Crystallogr. **A44**, 396 (1988).

[16] S. T. Picraux and J. U. Anderson, Phys. Rev. **186**, 267 (1969).

[17] N. M. Butt, J. Bashir, and M. Nasir Khan, Acta Crystallogr., Sect. A: Found. Crystallogr. **A49**, 171 (1993).

[18] S. D. Mukherjee, Phys. Lett. **64A**, 453 (1978).

[19] J. A. van den Berg and D. G. Armour, Nucl. Instrum. Methods **153**, 99 (1978).

[20] D. V. Morgan, in *Channeling—Theory, Observations and Applications* (Ref. 7), p. 99.